

First results on GOMOS/ENVISAT

J.L. Bertaux^{a,*}, A. Hauchecorne^a, F. Dalaudier^a, C. Cot^a, E. Kyrölä^b, D. Fussen^c,
J. Tamminen^b, G.W. Leppelmeier^b, V. Sofieva^b, S. Hassinen^b, O. Fanton d'Andon^d,
G. Barrot^d, A. Mangin^d, B. Théodore^d, M. Guirlet^d, O. Korablev^{a,g}, P. Snoeij^e,
R. Koopman^e, R. Fraisse^f

^a Service d'Aéronomie du CNRS/IPSIL, BP. 3, 91371 Verrières-le-Buisson, France

^b Finnish Meteorological Institute, P.O. Box 503, FIN-00101 Helsinki, Finland

^c Belgian Institute for Space Aeronomy, 3 av. Circulaire, B-1180 Brussels, Belgium

^d ACRI-ST, 260 Route du Pin Montard, BP. 234, 06904 Sophia Antipolis, France

^e European Space Agency, Estec, Esrin, Postbus 299, 200 AG Noordwijk, The Netherlands

^f Astrium EADS, 31 Avenue des Cosmonaute, 31402 Toulouse Cedex 4, France

^g Space Research Institute (IKI), 84/32 Profsoyuznaya, 117810 Moscow, Russia

Received 1 December 2002; received in revised form 27 August 2003; accepted 1 September 2003

Abstract

Global ozone monitoring by occultation of stars (GOMOS) on ENVISAT is the first space instrument dedicated to the study of the atmosphere of the Earth by the technique of stellar occultations (global ozone monitoring by occultation of stars). From a polar orbit, it allows to have a good latitude coverage. Because it is self-calibrated, it is particularly well adapted to the long time trend monitoring of stratospheric species. With four spectrometers the wavelength coverage of 245–942 nm allows to monitor ozone, H₂O, NO₂, NO₃, air, aerosols, O₂ and the temperature profiles. Two additional fast photometers (1 kHz sampling rate) allow for the correction of scintillations, as well as a study of the turbulence regime. A high vertical resolution profile of the temperature may also be obtained from the time shift between the red and the blue photometer. The first results of GOMOS are presented and ozone measurements compared to other sources.

© 2003 COSPAR. Published by Elsevier Ltd. All rights reserved.

Keywords: Atmosphere; Ozone; Occultation; Stellar occultation; Stratosphere

1. Introduction

Global ozone monitoring by occultation of stars (GOMOS) is one of three instruments with Michelson interferometer for passive atmospheric sounding (MIPAS) and scanning imaging absorption spectrometer for atmospheric cartography (SCIAMACHY) that the European Space Agency has selected to fly in space on ENVISAT platform, in order to collect the corpus of ozone data (and other atmospheric parameters) necessary to answer the following questions:

- What is the time evolution of ozone in the stratosphere (the trend) all over the world?
- What is the effect of CFCs release limitations?
- Is the measured ozone trend equal to the trend predicted by our best simulation model predictions?
- If not, is there anything in the data that can indicate where are the shortcomings of our models and how can they be improved for more reliable predictions?

Among the three instruments devoted to atmospheric chemistry, the particular role of GOMOS is to establish the 3-D distribution of ozone in the stratosphere and to monitor its trend as a function of altitude, thanks to the particularly high absolute accuracy offered by the occultation of stars. GOMOS is the acronym of global ozone monitoring by occultation of stars, and was first proposed to ESA by a group of European scientists

* Corresponding author. Tel.: +33-1-6447-4251; fax: +33-1-6920-2999.

E-mail address: bertaux@aerov.jussieu.fr (J.L. Bertaux).

(Bertaux et al., 1988). It is the first space instrument specially designed and built to perform atmospheric measurements by stellar occultations: the UVISI instrument (ultraviolet and visible imagers and spectrometers) on the Midcourse Space Experiment (MSX), which already provided very interesting results with this technique (Yee et al., 2002), was not designed for this purpose, and required that the full spacecraft be oriented to the star, while GOMOS has a moving mirror which is oriented successively to the various stars to be occulted.

GOMOS is implemented on ENVISAT opposite to the velocity vector, allowing to look near the horizon the successive setting down of various stars while the platform is moving along its orbit. The principle of the stellar occultation is quite simple (Hays and Roble, 1968). When the star is high above the horizon, the light spectrum of the star $S_0(\lambda)$ is recorded by GOMOS, free of any atmospheric absorption. A few seconds later, the light spectrum of the same star seen through the atmosphere (just above the horizon) is again recorded. The spectrum $S(\lambda, z)$ is modified by the absorption of all atmospheric constituents integrated over the line of sight from ENVISAT to the star, according to the Beer–Lambert law:

$$S(\lambda, z) = S_0(\lambda) \exp(-\sigma_\lambda N(z)), \quad (1)$$

where λ is the wavelength, z is the altitude of the line of sight above the horizon, $N(z)$ (mol/cm^2) is the integrated quantity of ozone along the line of sight (slant density) and σ_λ the absorption cross section of ozone. Here, only ozone absorption is considered for clarity.

From Eq. (1) one derives:

$$N(z) = -\frac{1}{\sigma_\lambda} \log \frac{F(\lambda, z)}{F_0(\lambda)}. \quad (2)$$

During one single occultation, a series of tangential column (slant) densities are obtained at various altitudes z_j . This series can be inverted (vertical inversion) to yield the vertical distribution of the local density of O_3 (mol/cm^3), assuming that the atmosphere is locally spherically

symmetric. This vertical inversion is straightforward with the so-called onion-peeling technique.

Besides the extreme simplicity of the retrieval algorithm when compared to other methods, the occultation technique has one enormous advantage readily expressed from the mathematical form of Eq. (2): an absolute estimate of $N(z)$ is obtained from the ratio of two measurements taken with the same instrument at a few seconds of interval. The method is inherently self-calibrated, and even if the spectral sensitivity of the instrument is changing with time, the ratio will be measured correctly and hence the column density $N(z)$. This protection against long-term drift is of course ideal for the study of trends of ozone and other constituents. The primary measurement of GOMOS is this ratio, which is the spectral transmission of the atmosphere as a function of the tangential altitude of the line of sight. Within the spectral range of GOMOS (Table 1), O_3 , NO_2 , NO_3 , OCIO , H_2O , O_2 aerosols and temperature may be measured as a function of altitude. Night side measurements are preferred, because on the day side, the bright limb intensity is competing with the stellar flux; the detectors are charge coupled devices (CCD), and two CCD groups of lines are devoted to the limb brightness, to be subtracted from the CCD lines collecting the star's spectrum. Here we will report only on night side measurements.

ENVISAT was launched with Ariane 5 on March 1st, 2002, and GOMOS obtained its first occultation of a star on March 20. Since then, it operated smoothly, and collected more than 27,000 occultations by the end of August 2002.

Some GOMOS instrument parameters are summarized in Table 1. GOMOS includes two spectrometers with 4 CCDs, and two fast photometers to measure scintillations and to correct the transmission spectra from the deformations produced by the chromatic refraction. The star tracker maintains the star image at the focus of the telescope, inside a slit which size is equivalent to 10 spectral pixels. The spectral resolution is better than 2 pixels.

Table 1
GOMOS instrument parameters

Optical performance parameters	Channel	Spectral range	Spectral sampling per pixel
	UV–Vis	250–675 nm	0.31 nm
	IR1 (O_2)	756–775 nm	0.05 nm
	IR2 (H_2O)	926–952 nm	0.05 nm
	Phot 1 (blue)	650–700 nm	Broad band
	Phot 2 (red)	470–520 nm	Broad band
Altitude range	Minimum: 5–18 km (night), 25 km (day)	Maximum 250 km	
Vertical resolution	1–1.7 km (0.5 s sample)		
Operation	Continuous over orbit		
Data rate	222 kb/s		
Mass	163 kg		
Power	146 W		

2. Reference stellar spectra and spectral transmission

At each occultation, when the star is acquired and tracked by the star acquisition and tracking unit (SATU), at high altitude (usually around 120 km), the five first spectra are averaged together to give the reference star spectrum S_0 , outside the atmosphere. Fig. 1 represents spectra for various stars, illustrating two features of GOMOS. The first feature is that the signal is dimmer when the star magnitude is larger (the magnitude of a star is defined according to its flux at 550 nm). Of course, brighter stars are favoured in the selection of stars, but in order to get a good latitude coverage, one has to select quite often dimmer stars (up to magnitude 3), by lack of bright stars at a given latitude. Obviously, the accuracy of ozone (and other species) retrieval depends on the star brightness. The second feature is the fact that hot stars have much more UV flux than cool stars of equal magnitude, allowing ozone retrieval with the Hartley’s absorption continuum, peaking at 250 nm (the shortest wavelength of GOMOS). Each spectrum is measured for 0.5 s, and the signal per pixel in electrons gives the indication of the shot noise, the main source of error bar for the spectral transmission: 1% for a signal of 10,000 electrons. The pixel spectral size is given in the last column of Table 1.

Note in Fig. 1 the strong Fraunhofer hydrogen lines in the spectrum of star S005 (GOMOS identification number of the star Vega, the 5th brightest in the sky), allowing a good in-flight wavelength calibration of the spectrometer, and a relative lack of signal around 380 nm

nm, where the spectrum of the star produced by a holographic grating is divided in two parts, reaching two different CCDs with some resulting vignetting.

In Fig. 2 are plotted the spectral transmission T_m at a number of tangent altitudes z during one occultation of star Sirius (the brightest in the sky). $T_m(z)$ is obtained by ratioing $S_m(z)/S_0$, where $S_m(z)$ is the measurement of the spectrum through the atmosphere obtained at altitude z , during 0.5 s (altitude integration over 1.7 km at most, depending on the distance of the star to the orbital plane). In this particular case, the minimum altitude was lower than 10 km, while for dimmer stars, the tracker may lose the star between 20 and 10 km. Note the gap of data 380–405 nm, where the spectrometer instrumental vignetting occurs. In the future, this gap will be eventually filled, because there is still some flux (Fig. 1). From UV to 700 nm, one can recognize on the transmission spectra:

- the strong Hartley’s absorption continuum at 250–280 nm, allowing to measure ozone up to 100 km,
- the Huggins bands of ozone at 300–340 nm (visible at 25, 30 and 36 km),
- small spectral features around 440 nm due to NO_2 ,
- the broad absorption Chappuis band of ozone, from 480 to 700 nm, with pronounced spectral features,
- a small O_2 band at 680 nm,
- the Rayleigh extinction of air, giving the slope around 400 nm (visible essentially below 30 km).

In Figs. 3 and 4 are displayed the spectral transmission obtained respectively in the O_2 band (called the A band) around 760 nm, and in the water vapour band

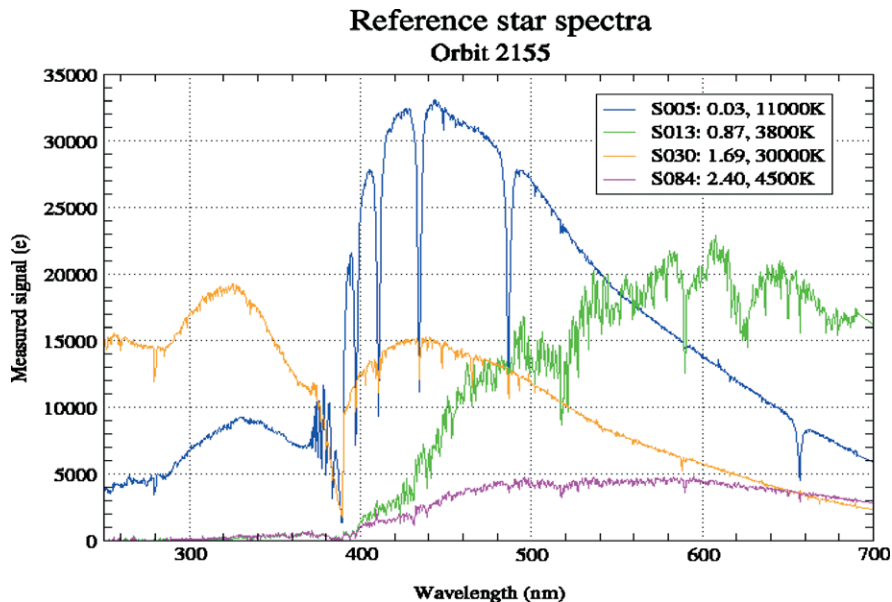


Fig. 1. Spectra of different stars observed by GOMOS. Hot stars contain more UV light than cool stars and are more suitable to the measurement of mesospheric ozone. Just below 400 nm, the low signal is due to the separation of the spectrum on two CCDs. In the panel are indicated the GOMOS starcatalogur number (I.E., S005), the visual magnitude, and the color temperature of the star.

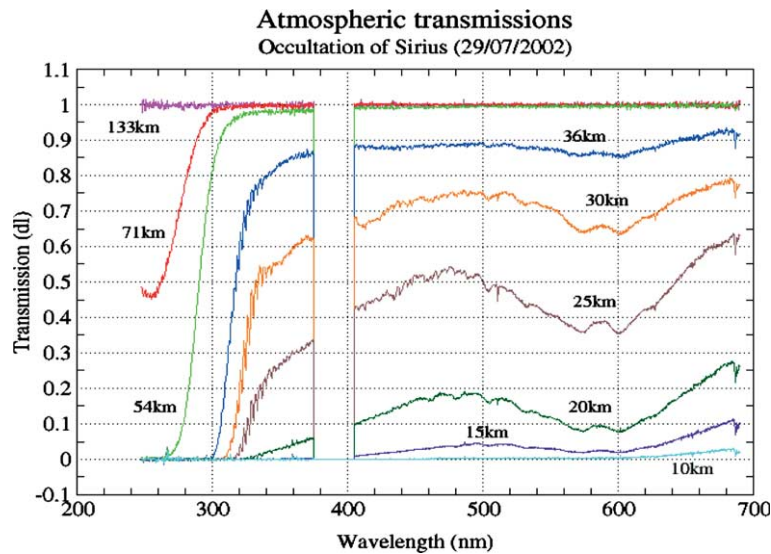


Fig. 2. Atmospheric transmission spectra along the line of sight from GOMOS to star Sirius, for different tangent altitudes.

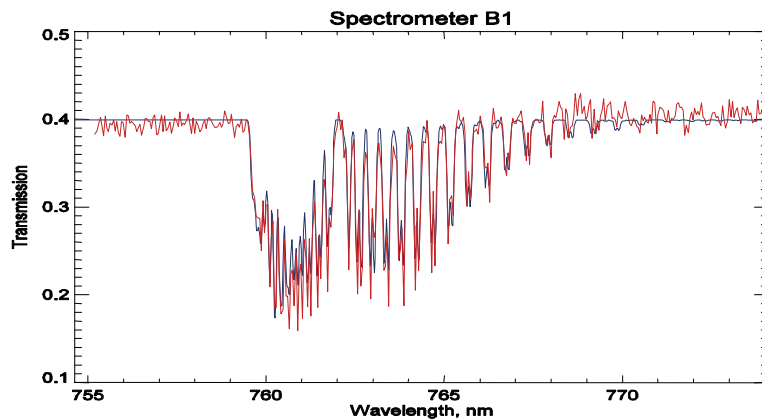


Fig. 3. Spectral transmission measured in the O₂ band (called A band around 760 nm), compared with a HITRAN model (adjusted to the baseline).

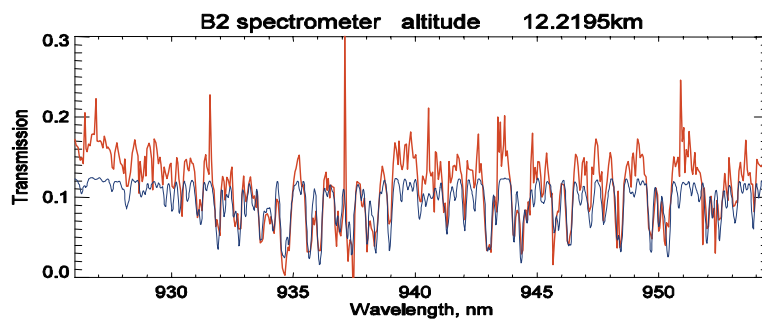


Fig. 4. Spectral transmission measured in the H₂O band at 12.2 km of altitude, compared with a HITRAN model (adjusted to the baseline).

around 936 nm. Transmission spectra are compared with HITRAN line-by-line calculations of the model transmission T_{mod} . It should be noted the high degree of resemblance between the data and the model, demonstrating the high spectral quality of the data, considering the weakness of the stellar source.

3. Spectral and vertical inversion

The data retrieval, performed independently for each occultation, is a two step process: the spectral inversion allows to retrieve the line densities (local densities integrated along the line of sight) of all absorbing species for

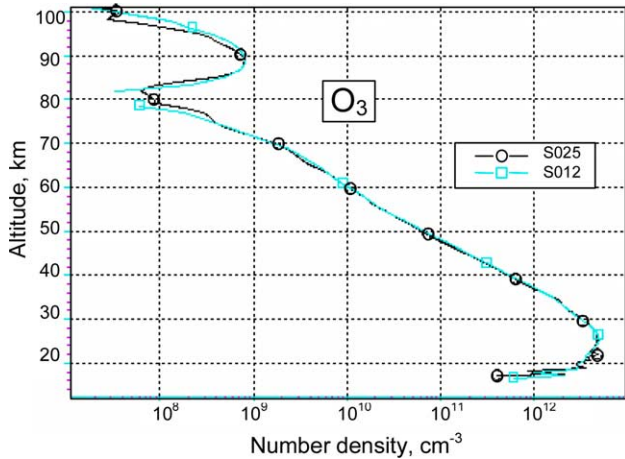


Fig. 5. Two vertical profile of ozone obtained at the same geographical location, but at two different (successive) orbits, and using two different stars with the tangent points differing by only 25 km.

each measurement of the transmission during the occultation, while the vertical inversion retrieves the vertical distribution of the local densities from the series of the line density measurements produced by the spectral inversion.

For the spectral inversion of the UV–Vis spectra of Fig. 2, a Levenberg–Marquardt best fit process minimizes the χ^2 between the measured spectrum T_m and a model T_{mod} , computed with ozone, NO_2 , NO_3 , air, and aerosols line (slant) densities as unknowns. Before the fit is performed, a correction to the spectrum is applied to

take into account the scintillation of the star, produced by the fine structure of the temperature distribution of the atmosphere. Scintillations are measured with the two photometers at 1 kHz rate, and observed scintillations, which are different between the blue and the red (because the index of refraction changes with wavelength) allow to perform this correction. It was found that the correction was not perfect, resulting in a corrected spectrum T_{cor} which cannot be fitted perfectly (within the data noise) by any combination of the unknowns: there are residuals $T_{cor} - T_{mod}$ which may amount sometime to 0.01–0.02, over several nanometers. The amount of these residuals are variable from one occultation to the next; they peak around 30 km, and seem negligible below 20 km and above 40 km.

One way to check the internal consistency of the GOMOS data and retrieval scheme is to compare the vertical profile of ozone obtained at the same geographical location, but at two different (successive) orbits, and using two different stars (at two consecutive orbits, the same star is occulted at the same latitude, but at longitudes differing by about 25°). This was done in Fig. 5, where the tangent points of two consecutive orbits was differing by only 25 km. The two vertical profiles are in excellent agreement, and show also the unique capability of GOMOS to measure mesospheric ozone at night. It should be noted that, while it is assumed, in the vertical inversion, that the ozone distribution is locally spherically symmetric, in reality there are horizontal variations of the local density. As a result, the line density integrated at a given tangent altitude

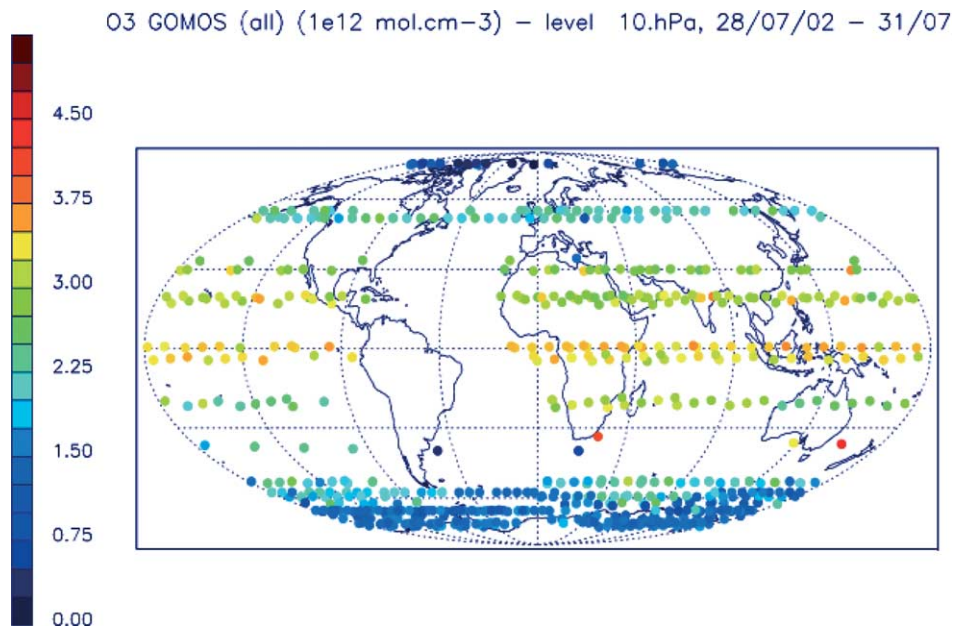


Fig. 6. Geographical distribution of the GOMOS measurements obtained over 3 days, with the local density at a constant level (here, 10 hPa) color-coded (in units of 10^{12} mol/cm $_3$). Each point corresponds to one single star occultation.

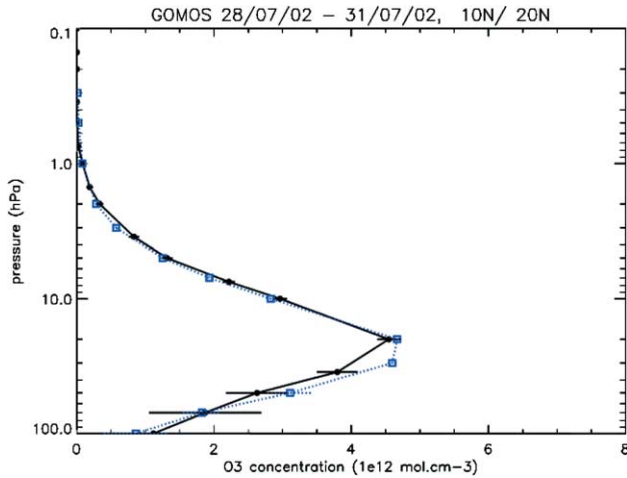


Fig. 7. Average GOMOS ozone profile for a latitude band 10–20 N obtained over 3 days, compared with the vertical profile of the Fortuin–Kelder climatology (blue); the dispersion bar attached to the GOMOS results is the 1 sigma dispersion of all the GOMOS measurements in this range of latitude and altitude.

may depend on the angle of the line of sight (with the meridian circle, for example). Calculations have shown that there may be 4% variation in a modelled ozone 3D field, and this may account for some of the small differences seen in the two profiles of Fig. 5.

4. Comparison of GOMOS ozone measurements with ozone climatology

A series of GOMOS ozone measurements over 4 days in July 2002 have been compiled and compared to the climatology of Paul et al. (1998), referred as F–K climatology in the following. Fig. 6 illustrates the geographical distribution of the GOMOS measurements, with the local density color-coded. In Fig. 7, the average GOMOS profile for a latitude band 10°N–20°N is compared with the vertical profile of the F–K climatology; the dispersion bar attached to the GOMOS results is the 1 sigma dispersion of all the GOMOS

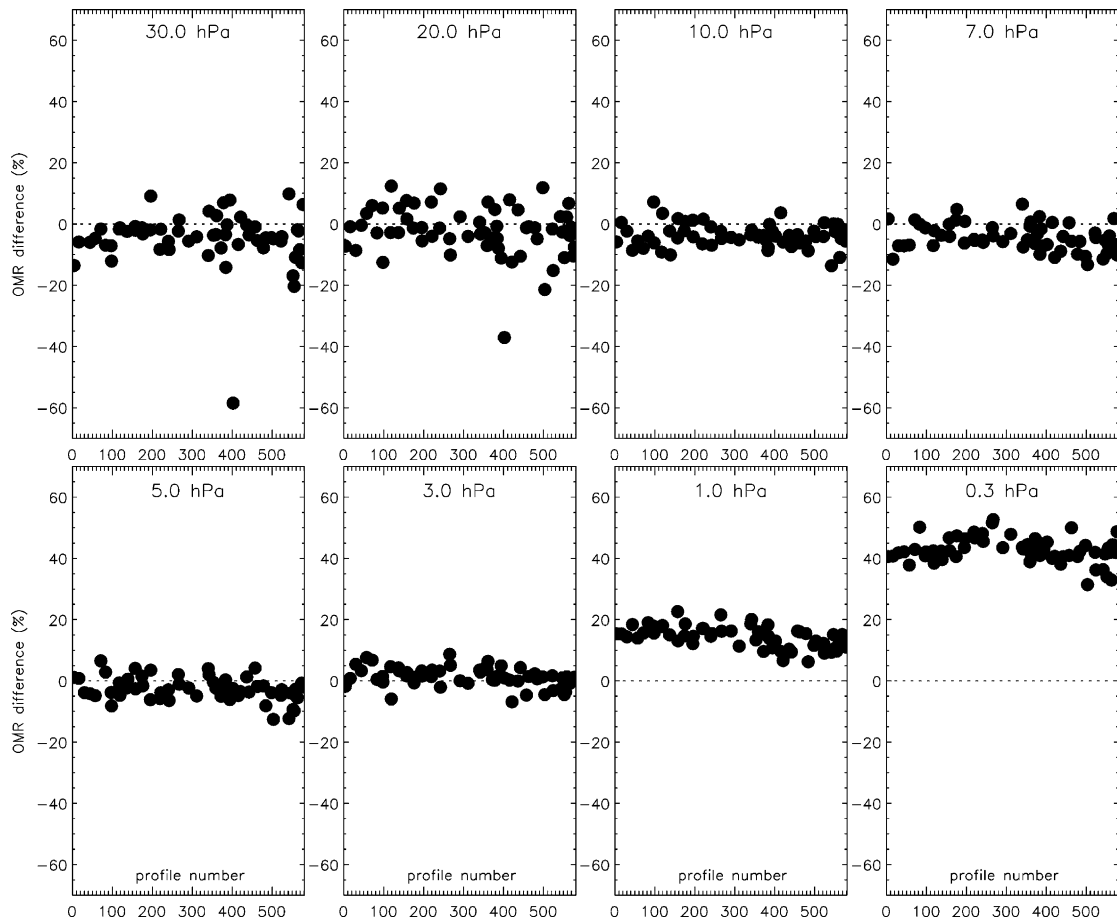


Fig. 8. Individual GOMOS measurements at various level pressure are plotted according to profile number (over 4 days), with the ordinates displaying the relative difference with the reference density of the Fortuin–Kelder climatology. The dispersion of GOMOS is highest at 20 hPa, reflecting natural variability at this altitude, while at other pressure levels the dispersion is within a few percent, giving a maximum upper limit of the GOMOS error. At the two highest level of 1 and 0.3 hPa, GOMOS is higher than climatology most likely due GOMOS night side measurements, while the climatology reflects also day side measurements.

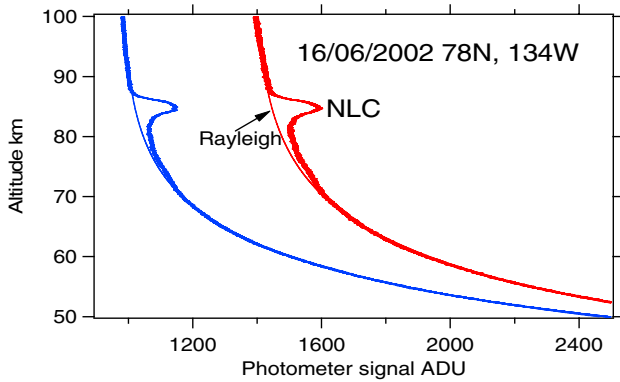


Fig. 9. Example of GOMOS photometers observation of a noctilucent cloud (or polar mesospheric cloud), detected as an increase of solar light by the particles of the clouds, in addition to the Rayleigh scattering by air molecules around 85 km. The lower signal is the blue photometer, and the higher is the red photometer (in engineering ADU, Analog to Digital Unit).

measurements in this range of latitude and altitude (65% of all measurements are within this dispersion from the average). The agreement is excellent. In Fig. 8, the individual GOMOS measurement at various level pressure are plotted according to profile number (over 4 days), with the ordinates displaying the relative difference with the reference density of the F–K climatology. The dispersion of GOMOS is highest at 20 hPa, reflecting natural variability at this altitude, while at other pressure levels the dispersion is within a few percent, giving a maximum upper limit of the GOMOS error. There is an obvious strong difference at the two highest level of 1 and 0.3 hPa, respectively of +15% and +40% for GOMOS w.r.t. the climatology. This is most likely due to the fact that the present analysis was restricted to the night side, while the climatology reflects also day side measurements.

5. Noctilucent clouds (polar mesospheric clouds)

In Fig. 9 is shown an example of GOMOS photometers observation of a noctilucent cloud (or polar mesospheric cloud), detected as an increase of solar light by the particles of the clouds, in addition to the Rayleigh scattering by air molecules. The spectrometers have also seen this emission, and with bright stars they could be seen also in absorption. Comparing spectral emission and absorption will allow to determine the characteristics (at least the size distribution) of these icy particles.

Also, a statistical analysis of PMC occurrence will be established. In order to condense, the icy particles need some water vapour and a very cold temperature, conditions found only in the high latitude summer mesosphere. It has been suggested (Thomas, 1991) that they could be a potential indicator of global atmospheric changes: the increase of CO₂ will decrease the temperature at these altitudes (by IR radiative cooling), while at the same time there might be an increase of water vapour injection in the stratosphere.

Acknowledgements

ENVISAT is a space mission of ESA, and GOMOS has been built by Astrium company under the direction and funding from ESA. We are particularly grateful to Jacques Louet and Guido Levrini from ESTEC for their efforts to establish the ENVISAT programme, to Alex Popescu, Thorgeir Paulsen, Kurt Lengen, Chris Reading, Tobias Wehr at Estec, Lidia Saavedra, Marta de Laurentis at Esrin, Alain Clochet, Jacques Dauphin and Patrick Uguen at Astrium, Nicole Papineau and Carole Deniel at CNES, and national funding agencies from France (CNES), Finland (TEKES), and Belgium for supporting partially the data analysis. We wish to thank also Jean-Claude Lebrun, Françoise Pinsard, Laurent Blanot, François Bougnet and Stéphane Marchand for their help at Service d'Aéronomie du CNRS.

References

- Bertaux, J.L., Pellinen, R., Simon, P., Chassefière, E., Dalaudier, F., Godin, S., Goutail, F., Hauchecorne, A., Le Texier, H., Mégie, G., Pommereau, J.P., Brasseur, G., Kyrola, E., Tuomi, T., Korpela, S., Leppelmeier, G., Visconti, G., Fabian, P., Isaksen, S.A., Larsen, S.H., Stordahl, F., Cariolle, D., Lenoble, J., Naudet, J.P., Scott, N., GOMOS, proposal in response to ESA EPOP-1, A.O.I, January 1988.
- Hays, P.B., Roble, R.G. Stellar spectra and atmospheric composition. *J. Atmos. Sci.* 25, 1141, 1968.
- Paul, J., Fortuin, F., Kelder, H. An ozone climatology based on ozone sonde and satellite measurements. *J. Geophys. Res.* 103, 31709–31734, 1998.
- Thomas, G.E. Mesospheric clouds and the physics of the mesopause region. *Rev. Geophys.* 29, 553–575, 1991.
- Yee, J.-H., et al. Atmospheric remote sensing using a combined extinctive and refractive stellar occultation technique I. Overview and proof-of-concept observations. *J. Geophys. Res.* 107 (D14), 4213, 2002.